

Research Article

## Capillary Suction Properties of Mortar Made with Recycled Plastic Aggregates Elaborated from Waste Electrical and Electronic Equipment

Jeronimo Kreiker <sup>1,\*</sup>, Melina Gomez <sup>2,†</sup>, Lucas Peisino <sup>1,†</sup>, Nelio Ochoa <sup>2,†</sup>, Belen Raggiotti <sup>3,†</sup>

1. Centro Experimental de la Vivienda Económica, CEVE-CONICET, AVE, Igualdad 3585 X5003JMB, Córdoba, Argentina; E-Mails: [jkreiker@ceve.org.ar](mailto:jkreiker@ceve.org.ar); [jerokreiker@gmail.com](mailto:jerokreiker@gmail.com); [lpeisino@gmail.com](mailto:lpeisino@gmail.com)
2. Instituto de Física Aplicada, INFAP-CONICET, UNSL, Almirante Brown 869, D5700ANU, San Luis, Argentina; E-Mails: [dimelinag@gmail.com](mailto:dimelinag@gmail.com); [aochoa@unsl.edu.ar](mailto:aochoa@unsl.edu.ar)
3. Centro de Investigación, Desarrollo y Transferencia de Materiales y Calidad (CINTEMAC), UTN–FRC, Maestro M. López y Cruz Roja Argentina, Córdoba, Argentina; E-Mail: [belenraggiotti@gmail.com](mailto:belenraggiotti@gmail.com)

† These authors contributed equally to this work.

\* **Correspondence:** Jeronimo Kreiker; E-Mails: [jkreiker@ceve.org.ar](mailto:jkreiker@ceve.org.ar); [jerokreiker@gmail.com](mailto:jerokreiker@gmail.com)**Academic Editor:** José Ignacio Álvarez Galindo**Special Issue:** [New Trends on Construction Technologies and Sustainable Building Materials](#)*Recent Progress in Materials*  
2024, volume 6, issue 1  
doi:10.21926/rpm.2401007**Received:** October 18, 2023  
**Accepted:** March 06, 2024  
**Published:** March 15, 2024

### Abstract

It is possible to revalue the plastic fraction from WEEE using it as a recycled aggregate (RA) in cement mortars. However, this feasibility depends on elaborating a granular material via a core-shell strategy to stabilize the potential contaminants. The core is a plastic particle, and the shell is a cement, fillers, and activated carbon mixture. Due to the hydrophilic characteristics of the shell and the presence of interstitial sites generated by the use of the RA, it is necessary to study the wetting properties of these mortars. This article presents the results of capillary suction and contact angle studies of mortars made with RA having different shell compositions. The capillary suction of the latter is higher than in traditional mortars, which limits their use for structures exposed to water and environmental agents but opens



© 2024 by the author. This is an open access article distributed under the conditions of the [Creative Commons by Attribution License](#), which permits unrestricted use, distribution, and reproduction in any medium or format, provided the original work is correctly cited.

the possibility of new uses in permeable concrete or for the manufacture of building components.

### **Keywords**

Recycled aggregate; plastic from WEEE; sustainable building components; capillary suction

## **1. Introduction**

Shredded recycled plastic as a total or partial replacement for natural aggregates in cement mortars has been extensively studied. The chemical nature of the polymers, their dosage, shape, and size are the main factors that influence the physical and mechanical properties of the mortar and limit or promote its use depending on the demands of the application [1]. The thermal insulation properties may improve with plastic aggregates due to their lower density [2]. However, there is a general decrease in mechanical strength, except when reinforcing fibers are incorporated to enhance flexural properties [3]. On the other hand, plastic aggregates modify capillary suction by altering the hydrophobicity of the aggregate, thereby changing the wetting characteristics of the mortar [4]. This property is significant for the durability of mortars, which depends on the entry of external agents through transport phenomena that occur inside their porous structure [5]. On the other hand, foamed concretes have found various uses in civil engineering. This type of concrete is achieved through various foaming agents or physical methods, and depending on the type of foaming agent used, materials with diverse physical, mechanical, and wetting properties are obtained, thus expanding the possibilities of application [6].

Our research team developed a technology to replace sand using plastics from waste electrical and electronic equipment (WEEE) as aggregate [7]. This type of plastic, composed mainly of Acrylonitrile-butadiene-Styrene (ABS), High Impact Polystyrene (HIPS), and Polycarbonate (PC), cannot be added directly to cement because it contains brominated flame retardants (BFRs) [8]. In previous work, we reported that these BFRs leach in an alkaline Portland cement medium, evidenced by a yellow coloration in the mortar [9, 10]. This technology involves the core-shell strategy, in which the recycled plastic core is coated with successive layers of Portland cement and additives to yield a recycled plastic aggregate (RPA) (Figure 1). Thus, inhibiting the leaching of BFRs made it possible to use this plastic waste as aggregate in mortars. Aggregates with an average diameter of 3 mm and 8 mm were prepared and used as aggregates to mold bricks, blocks, and plates, replacing natural sand. These building components have excellent physical and mechanical properties [8]. However, in order to promote the use of building components made with this RPA or the utilization of this aggregate in total or partial replacement of sand in mortars and concrete structures, it is necessary to learn about the porous structure and the capillary suction properties of mortars manufactured with this RPA.



**Figure 1** Recycled Plastic Aggregate (RPA).

This paper presents the results of studies on the capillary suction capacity and contact angle of specimens made with 3 mm and 8 mm RPAs containing different types of activated carbon as stabilizing additives. Based on the results obtained, we can propose using this material for mortars that do not require low moisture permeability, which could deteriorate the structure.

## 2. Materials and Methods

The different aggregates used in this study are listed in Table 1. The aggregate of entry 1 corresponds to a conventional natural aggregate (NA), fine river sand. In entries 2 and 3, aggregates of crushed plastics from WEEE (FPR) are presented in two different sizes (FPR#3 = 3 mm and FPR#8 = 8 mm). Entries 4 and 5 present the aggregates developed by our research group via the core-shell strategy, obtained from encapsulating these plastic particles with ordinary Portland cement (OPC) and inert additive (FPR#3@OPC:PPR and FPR#8@OPC:PPR). Finally, entries 6, 7, 8 and 9 present aggregates formed by the encapsulation of plastic with Portland cement, inert additive and activated carbon (FPR#3@OPC:PPR:CA/MMF, FPR#8@OPC:PPR:CA/MMF, FPR#3@OPC:PPR:CA/CB and FPR#8@OPC:PPR:CA/CB); in this case, two different activated carbon types were used (MMF and Clarisorb B).

**Table 1** Aggregates composition.

Entry	Samples	Shell composition	Activated carbon (name - % of mass)	$\rho$ (g/cm <sup>3</sup> )
1	NA (standard)	-	-	1.48
2	FPR#3	-	-	0.54
3	FPR#8	-	-	0.57
4	FPR@OPC:PPR#3	OPC + PPR	-	0.84
5	FPR@OPC:PPR#8	OPC + PPR	-	0.84
6	FPR@OPC:PPR:AC#3 (MMF)	OPC + PPR + CA	MMF-4.3	0.67
7	FPR@OPC:PPR:AC#3 (MMF)	OPC + PPR + CA	MMF-4.3	0.69
8	FPR@OPC:PPR:AC#3 (CB)	OPC + PPR + CA	Clarisol B-4.3	0.74
9	FPR@OPC:PPR:AC#3 (CB)	OPC + PPR + CA	Clarisol B-4.3	0.80

The samples' apparent density ( $\rho$ ) was obtained according to the IRAM 1733 standard [11]. The samples were placed in a known volume (100 cm<sup>3</sup>) and introduced in an oven until constant temperature. Then, with the data obtained, the density was calculated in grams over cm<sup>3</sup>.

These aggregates were then used to elaborate different cement mortar specimens according to the dosages shown in Table 2. Specimens of 4\*4\*16 cm were elaborated following the procedure described in the IRAM 1622:05 norm [12]. The aggregate used was fine river sand to make a STANDARD specimen, as shown in Table 2. The aggregate-to-cement ratio studied was 6:1. The water-to-cement ratio was close to 0.5 when FPR or RPA were the aggregates and 0.7 for sand. The specimens were cured for 60 days by water immersion at 25°C. After this time, the specimens were dried for two days at 50°C.

**Table 2** Mortar compositions and dosages.

Entry	Aggregate mass	Mass (g)	OPC (g)	Agg: OPC	Water (mL)	Mass total (g)	Total cement (g%) <sup>a</sup>	$\rho$ (g/cm <sup>3</sup> )
1	NA (standard)	379	50	6:1	36	429	50	12
2	FPR#3	131	50	6:1	26	181	50	28
3	FPR#8	300	70	6:1	60	370	70	23
4	FPR#3@OPC:PPR #3	169	50	6:1	25	219	96	44
5	FPR#8@OPC:PPR #8	239	55	6:1	60	294	143	59
6	FPR#3@OPC:PPR:CA/MMF	212	55	6:1	40	267	139	65
7	FPR#8@OPC:PPR:CA/MMF	219	55	6:1	50	274	144	65
8	FPR#3@OPC:PPR:CA/CB	238	55	6:1	40	293	157	65
9	FPR#8@OPC:PPR:CA/CB	231	55	6:1	40	286	152	65

<sup>a</sup> Total cement = OPC used to make Shell + OCP used to elaborate mortars.

The maximum capillary suction capacity was determined according to the IRAM 1871 norm [13]. This norm establishes a gravimetric method by determining the maximum capillary suction capacity using Equation 1.

$$C_{it} = \frac{M_{hit} - M_{si}}{A_i} \quad (1)$$

Where  $C_{it}$  is the increase in mass per unit area of the cross-section of the specimen at the time of reading (t) in grams per square meter,  $M_{hit}$  is the wet mass of the specimen at the moment of reading (t) in grams,  $M_{si}$  is the dry mass of the specimen in grams, and  $A_i$  corresponds to the area of the cross-section of the specimen in square meters. The capillary suction rate in grams by square meter is the value of the increase in mass by unit area of the specimen's cross-section at the moment of reading, which corresponds to the moment in which the variation between two successive determinations of wet mass is less than 0.1%.

The sessile drop method was used to determine the contact angles of the samples. A vertical unidirectional drip system was used, employing a syringe to apply a drop of water on the surface of the samples. The drop was filmed with an Olympus Nano-Scope OMV-PAL optic system with a digital camera using a green background to improve the image's contrast. The video had two minutes, and

the frames corresponding to times 0, 30, 60, 90, and 120 s were extracted from the video. The photograph analysis was performed using the Drop analysis LB-ADSA plugin of the ImageJ software. Mortar porosity was determined using Equations 2, 3, and 4.

$$m_{Ad} = W_w - W_d \quad (2)$$

$$V_{H_2Oab} = \frac{m}{\rho} \quad (3)$$

$$Porosity = \frac{V_{H_2Oab}}{V_{sample}} \cdot 100 \quad (4)$$

Where  $m_{Ad}$  is the absorbed water weight,  $\rho$  is the water density,  $W_d$  is the dry mortar weight, and  $W_w$  is the constant weight of mortars after 2 h immersed in water. The water surface excess was gently removed with tissue paper.

The average area of surface pores on the face of the specimen that came into contact with water was determined using the ImageJ software. For this, photographs of the specimen's face to be analyzed were captured with a digital camera. Subsequently, the images were scaled and converted to a two-color mode (binary mode) using the software. The number of pores and area of each on the surface of the mortar in contact with water was determined. Then, the mean pore area and surface porosity were calculated using the Analyze function of the software.

Statistical data: Only two measurements of suction parameters were taken for each specimen. The results informed are the average of the individual measurements, and in all cases, the coefficient of variation (CV) was less than 2%.

### 3. Results and Discussion

The different treatments performed on the RPA do not allow for correlating the water absorption values with properties related to the FPR, as reported by other researchers [14, 15]. The Materials and Methods section describes all the samples' data. Table 3 shows the data for capillary suction capacity, capillary suction rate, and apparent surface porosity based on pore area for all cement mortars. As expected, standard mortar has the lowest water suction velocity and water suction capacity values, and the capillary suction rates for all probes exceed the limit established by the norm of  $4 \text{ g/m}^2 \cdot \text{s}^{1/2}$  for concrete exposed to wet environments. All mortars containing FPR had higher values than the standard due to the low adhesion between plastic particles and cement. Also, in Table 3, a general trend can be observed: as the water suction capacity values increase, the values of suction rates increase as well. Such behavior can be expected when the textural properties of the samples are similar.

**Table 3** Capillary suction capacity, capillary suction rate and apparent surface porosity based on pore area are shown for all mortars.

Sample	Capillary suction capacity $C_{it}$ ( $\text{g/m}^2$ )	Capillary suction rate ( $\text{g/m}^2 \cdot \text{s}^{1/2}$ )	Mean pore area ( $\text{mm}^2$ )	Apparent surface porosity
STANDARD	6185	4.65	0.12	4.84
FPR#3	17500	67.49	0.18	79.31

FPR#8	14563	31.62	0.48	14.96
FPR#3@OPC:PPR	17750	35.57	0.13	7.03
FPR#8@OPC:PPR	11688	22.81	0.54	8.17
FPR#3@OPC:PPR:CA/MMF	27375	42.05	0.09	3.21
FPR#8@OPC:PPR:CA/MMF	21188	36.98	0.03	6.73
FPR#3@OPC:PPR:CA/CB	14563	22.04	1.36	18.50
FPR#8@OPC:PPR:CA/CB	23688	44.26	0.47	19.34

We tried to find different correlations to explain these results related to several weight ratios: cement, plastic, or carbon. As mentioned above, the different treatments performed on the FPR lead to different textural properties. Despite this difficulty, it was possible to establish a correlation for FPR series #3 and #8. Figure 2 and Figure 3 show the suction rate data versus apparent surface porosity based on pore area for FPR#3 and FPR#8, respectively. For most mortars, the suction rate increases as the apparent surface porosity increases. However, samples FPR#3@OPC:PPR:CA/MMF and FPR#8@OPC:PPR:CA/MMF showed low porosity values with high suction rates. This behavior may be associated with the presence of inkwell-type pores. In such pores, the increased water suction capacity can increase the convective flow of the fluid by increasing the suction rate.

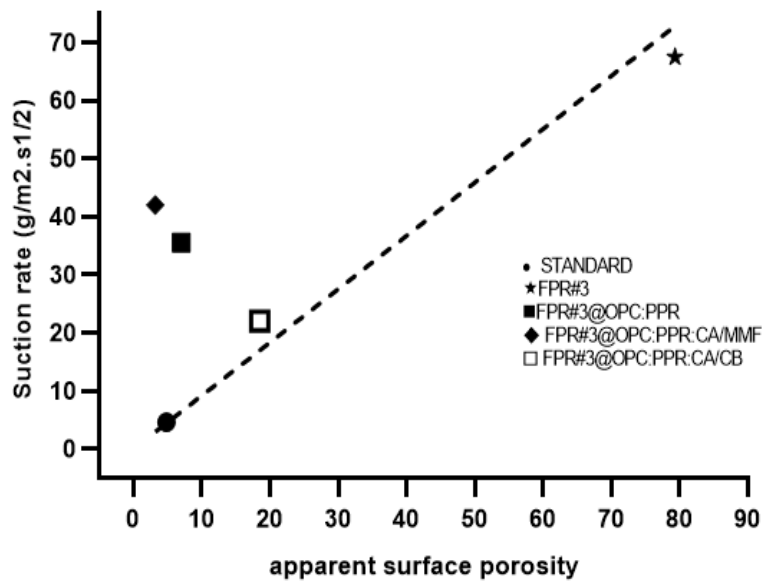


**Figure 2** Suction rate vs. apparent surface porosity in samples with FPR#3 as aggregate.

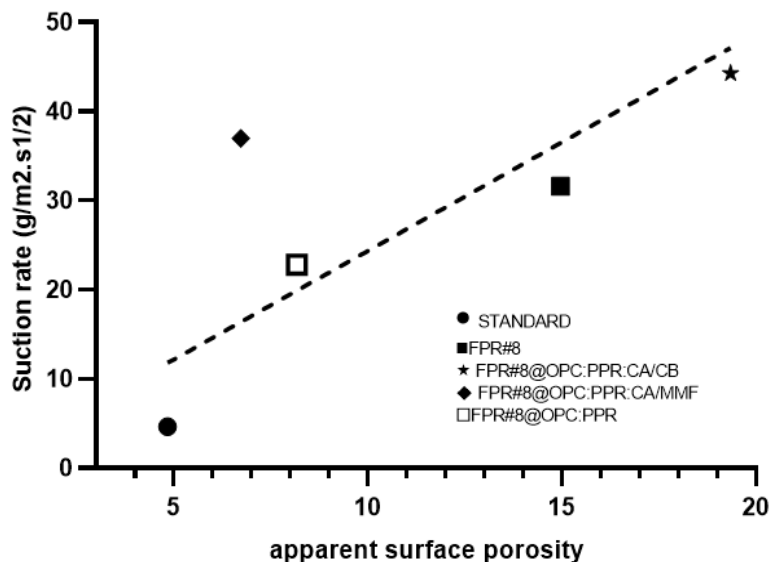


**Figure 3** Suction rate vs. apparent surface porosity in samples with FPR#8 as aggregate.

Contact angle measurements provide insight into changes in surface interaction with water. The contact angles measured as a function of time are detailed under Materials and Methods. It is well known that the value of the contact angle not only depends on the hydrophobicity of the surface but is also affected by other surface properties such as mean pore size, porosity, or roughness [16]. Therefore, it is useful to measure the contact angle at different times and extrapolate the value of the contact angle at time  $t = 0$  to reduce the error margin in the interpretation of the results. Table 4 shows the values of the contact angle (T) and the rate of decrease of the contact angle versus time.

**Table 4** Contact angles and their rate of decrease over time.

Sample	Time (seconds)					Contact Angle Rate of Decrease (°/s)
	0	30	60	90	120	
	Contact Angle (°)					
STANDARD	73.05	30.57	24.95	0	0	0.80
FPR#3	92.00	76.95	66.46	66.06	50.13	0.31
FPR#8	82.12	77.00	76.07	67.73	68.71	0.12
FPR#3@OPC:PPR	75.98	73.43	65.98	64.99	64.64	0.10
FPR#8@OPC:PPR	86.71	74.22	62.68	52.82	0	0.37
FPR#3@OPC:PPR:CA/MMF	84.11	22.62	0	0	0	2.04
FPR#8@OPC:PPR:CA/MMF	75.08	56.90	53.88	51.52	31.53	0.30
FPR#3@OPC:PPR:CA/CB	65.23	61.92	59.07	58.17	56.27	0.07
FPR#8@OPC:PPR:CA/CB	71.28	60.02	51.58	44.73	34.69	0.29

Standard mortar presents a contact angle value at an initial time of  $=73^\circ$ , and, as a general trend, the samples with FPR (FPR#3 and FPR#8) have contact angle values greater than  $75^\circ$ , indicating greater hydrophobicity. However, the samples with added activated carbon have contact angles similar to the standard sample. The results may arise from liquid penetration within the material, a

recently documented phenomenon impacting contact angle values for highly absorbent surfaces [17]. In the first few seconds, liquid intrusion into the material occurs, and the volume of the water droplet varies. Thus, highly absorbent mortars can generate important changes in the contact angle values, as shown by the samples with carbon aggregate. This phenomenon can be attributed to increased water imbibition within the carbons, thereby altering the liquid-surface interaction [18, 19].

Clarke et al. [20] studied the effect of water imbibition in membranes with different pore sizes and found that volume variation due to imbibition increased with pore size. In our study, the capillary suction rate is an indirect measure of water imbibition in mortars. However, since the nature of the components of the mortars varies, finding a correlation with the pore area is not straightforward. The results can be seen in the graph in Figure 4. Extrapolating the slope of the straight line from the origin of coordinates of the graph to the mean pore area and capillary suction rate values of the standard sample allows for the estimation of theoretical values in mortars with higher pore area values (while maintaining the same type of components as the standard mortar). Only two mortars fail to present capillary suction rates above these estimated values: FPR#8@OPC:PPR and FPR#3@OPC:PPR:CA/CB. In the case of the last sample, attaining a mortar with a reduced surface pore area while maintaining these components could significantly reduce its water absorption properties. Further work is in progress.

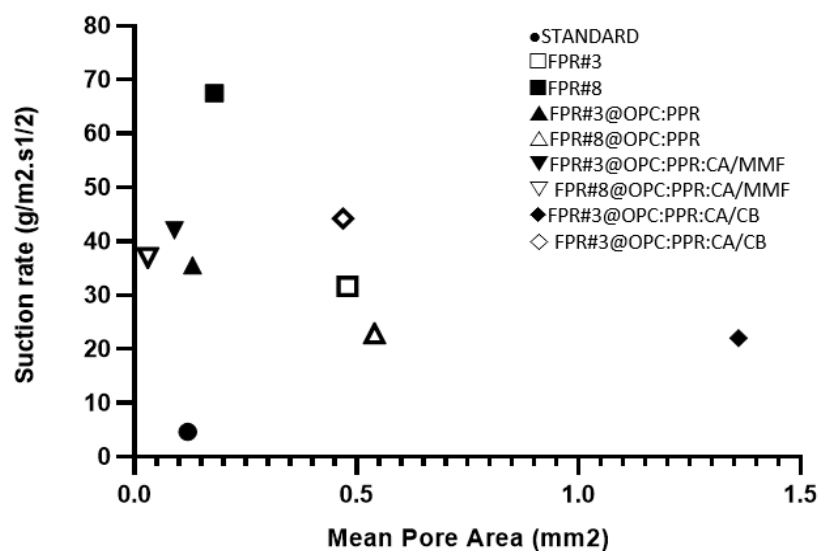


**Figure 4** Values of mean pore area and water absorption rate for all samples.

#### 4. Conclusions

- Using APR as aggregate to replace natural aggregates could be an interesting material for modifying cement mortar properties, such as the capillary suction capacity and the capillary suction velocity, without significantly affecting mechanical properties.
- For mortars where FPR was used in total replacement of the natural aggregate, water absorption is very high, probably due to voids at the interface between the cementitious matrix and the plastic aggregate because of the low cohesion of the particles. Although this effect should not occur with APR because cohesion occurs between the cementitious nature of the shell and the matrix of similar characteristics, very high values of capillary suction



capacity and velocity are also observed, probably due to the nature of the shell components and not to the porosity of the material, which was corroborated by the measurement of the contact angle in mortars with APR.

- Although mortars with APR showed high water absorption values and exceeded the limits established by the reference norms for mortar exposed to a wet environment, which affects the durability of the mortars, this limitation does not affect the potential use of building components such as blocks, bricks, and plates.
- The high permeability of mortars made with APR encourages their use in applications that require high water permeability, such as road or drain mortars.

## **Acknowledgments**

The authors wish to thank the National Council of Scientific and Technological Research (CONICET) and the Asociación Vivienda Económica (AVE). We are grateful to the Ministry of Science and Technology and Innovation, Argentine, for financial support for this research work. Melina Gomez. gratefully acknowledges the receipt of a fellowship from CONICET. We would like to thank D.I. Vanina Greppi and Dr. Julián González Laria for their support for the experimental phases of this research work.

## **Author Contributions**

Dr. Melina Gomez developed the experimental tasks related to capillary suction tests at INFAP. Dr. Jerónimo Kreiker, leads the research project on the recycling of plastics from WEEE and provides the funding for this research. Dr. Lucas Peisino, elaborated the test probes with different additives to carry out the experimental development at CEVE. Dr. Nelio Ocho directed the capillary suction experimental work at INFAP. Dr. Belen Raggiotti performed physical characterization of the RPA at CINTEMAC.

## **Funding**

The Ministry of Science, Technology and Innovation from Argentine and National Council of Scientific and Technological Research (CONICET) from Argentine provided financial support for this research work.

## **Competing Interests**

The authors have declared that no competing interests exist.

## **References**

1. Siddique R, Khatib J, Kaur I. Use of recycled plastic in concrete: A review. *Waste Manage.* 2008; 28: 1835-1852.
2. Gu L, Ozbakkaloglu T. Use of recycled plastics in concrete: A critical review. *Waste Manage.* 2016; 51: 19-42.

3. Ruiz-Herrero JL, Nieto DV, López-Gil A, Arranz A, Fernández A, Lorenzana A, et al. Mechanical and thermal performance of concrete and mortar cellular materials containing plastic waste. *Constr Build Mater.* 2016; 104: 298-310.
4. Saikia N, De Brito J. Use of plastic waste as aggregate in cement mortar and concrete preparation: A review. *Constr Build Mater.* 2012; 34: 385-401.
5. Marzouk OY, Dheilly RM, Queneudec M. Valorization of post-consumer waste plastic in cementitious concrete composites. *Waste Manage.* 2007; 27: 310-318.
6. Choudhury S, Jena T. Influence of surfactant on foam generation and stabilization in cement slurry. *Mater Today Proc.* 2023; 93: 340-345.
7. Taus VL. Análisis de la succión capilar en hormigones: Influencia de distintos parámetros de ensayo. Argentina: Universidad Nacional del Centro de la Provincia de Buenos Aires (UNCPBA); 2010.
8. Aldrian A, Ledersteger A, Pomberger R. Monitoring of WEEE plastics in regards to brominated flame retardants using handheld XRF. *Waste Manage.* 2015; 36: 297-304.
9. Peisino LE, Gómez M, Kreiker J, Gaggino R, Angelelli M. Metal leaching analysis from a core-shell WEEE plastic synthetic aggregate. *Sustain Chem Pharm.* 2019; 12: 100134.
10. Gómez M, Peisino LE, Kreiker J, Gaggino R, Cappelletti AL, Martín SE, et al. Stabilization of hazardous compounds from WEEE plastic: Development of a novel core-shell recycled plastic aggregate for use in building materials. *Constr Build Mater.* 2020; 230: 116977.
11. IRAM. IRAM 1733: Morteros para mampostería. Mortero endurecido. Determinación de la densidad aparente. Perú: IRAM. Available from: <https://catalogo.iram.org.ar/#/normas/detalles/1971>.
12. IRAM. IRAM 1622: Determinación de resistencias mecánicas. Perú: IRAM. Available from: <https://catalogo.iram.org.ar/#/normas/detalles/9268>.
13. IRAM. IRAM 1871: Método de ensayo para determinar la capacidad y la velocidad de succión capilar de agua del hormigón endurecido. Perú: IRAM. Available from: <https://catalogo.iram.org.ar/#/normas/detalles/9219>.
14. Mc Carter WJ, Ezirim H, Emerson M. Properties of concrete in the cover zone: developments in monitoring techniques. *Magazine of Concrete Research.* 1995; 27: 243-251. doi: 10.1680/mac.1995.47.172.243.
15. Taus VL. Análisis de la succión capilar en hormigones: Influencia de distintos parámetros de ensayo. Argentina: Universidad Nacional del Centro de la Provincia de Buenos Aires (UNCPBA); 2010.
16. Akçaözoglu S, Atiş CD, Akçaözoglu K. An investigation on the use of shredded waste PET bottles as aggregate in lightweight concrete. *Waste Manage.* 2010; 30: 285-290.
17. Cañete AF. Estudio de la hidrofobicidad y autolimpieza en materiales con nanotratamientos superficiales. Barcelona, Spain: Universitat Autònoma de Barcelona; 2013.
18. Frías M, Sánchez de Rojas, Rodríguez Largo MI. Novedades en el reciclado de materiales en el sector de la construcción: Adiciones puzolánicas. Proceedings of the II jornadas de investigación en construcción (Instituto de ciencias de la construcción "eduardo torroja"; 2008 May 22-24; Madrid, Spain. Actas de las Jornadas. H.1. Materiales: Cementos, morteros y hormigones. Available from: <https://docplayer.es/5671035-Novedades-en-el-reciclado-de-materiales-en-el-sector-de-la-construccion-adiciones-puzolanicas.html>.

19. Gallego Punzano J. Empleo de adsorbentes como aditivos en cementos: Caracterización y aplicación en la eliminación de contaminantes ambientales. Seville, Spain: Universidad de Sevilla; 2014.
20. Clarke A, Blake TD, Carruthers K, Woodward A. Spreading and imbibition of liquid droplets on porous surfaces. *Langmuir*. 2002; 18: 2980-2984.